A Novel Approach for Robust Model Predictive Control Applied to Switched Linear Systems Through State and Output Feedback

Luis Carvalho[a,*], Marcus V. S. Costa[a], Leonardo H. Macedo[b] and Elenilson V. Fortes[c]

[a] Federal Rural University of the Semi-Arid Region, Rua Francisco Mota, 572, Pres. Costa e Silva, 59625-900, Mossoró, RN, Brazil

[b] São Paulo State University, Avenida Brasil, 56, Centro, 15385-000, Ilha Solteira, SP, Brazil

[c] Goiás Federal Institute of Education, Science, and Technology, Av. Presidente Juscelino Kubitschek, 775, Residencial Flamboyant, 75804-714, Jataí, GO, Brazil

ARTICLE INFO

Keywords:
Linear matrix inequalities;
Model predictive control;
Output feedback;
Stable invariant ellipsoids;
State feedback;
Switched systems.

Abstract

This paper proposes a robust switched model-based predictive controller design for discrete linear systems with state constraints, inputs, and disturbances limited in norm. Modeled via linear matrix inequalities, the online and offline designs of the proposed control aim at minimizing the upper bound of the quadratic performance index for a horizon of infinite prediction associated with the state estimator and the switching rule, seeking to guarantee the robust stability for closed-loop systems. To this end, three theorems are formulated. To demonstrate the effectiveness of the control strategy, a comparative analysis is performed between the performance of the proposed model and a benchmark method. From the results, it is possible to conclude that the proposed method is promising in the scope of control of linear systems subject to switching, being more efficient than the benchmark for the stabilization and control of both numerical examples.

1. Introduction

Dynamic systems can be classified as linear or nonlinear. A system is said to be linear when the superposition principle can be applied to it, otherwise, the system is classified as nonlinear. In practice, most real systems are nonlinear, and the study and control of this type of plant is a recurring challenge in the literature [1].

For nonlinear problems, there is also the aggravating factor that, in some cases, it is not possible to apply certain control techniques. Therefore, it is necessary to use linearization methods to obtain linear models that describe the dynamics of the plant as accurately as possible [2]. However, the linearization methods available for this purpose are not always adequate, which consequently makes it difficult for the control synthesis [3].

An alternative to circumvent this problem is based on the concept of local linear models that compose a global nonlinear model. Such a method consists of linearizing the model for two or more operating ranges while preserving the nonlinear dynamics of the system. This enables the application of several control strategies, from gain scaling to switching between subsystems [4].

The main works covering the fundamental concepts of switched linear systems date from the early 2000s and are presented in Liberzon [5] and Liberzon and Morse [6]. Since then, the studies about this method have

[*] This work was supported by the Coordination for the Improvement of Higher Education Personnel (CAPES) – Finance Code 001 and the São Paulo Research Foundation (FAPESP), under grants 2015/21972-6 and 2018/20355-1. The authors would also like to thank the Federal Institute of Education, Science, and Technology of Goiás (IFG), the Federal Rural University of the Semi-Arid Region (UFERSA), and the Research Group on Automation and Control (GEAC), for their support in the production of this work.

[*] Corresponding author: Elenilson V. Fortes (e-mail: elenilson.fortes@ifg.edu.br).

E-MAIL(s):
francisco.costa32448@alunos.ufersa.edu.br (L. Carvalho);
marcus.costa@ufersa.edu.br (M.V.S. Costa);
leohfmp@ieee.org (L.H. Macedo);
elenilson.fortes@ifg.edu.br (E.V. Fortes)

ORCID(s):
0000-0002-1996-7815 (L. Carvalho);
0000-0002-2112-6433 (M.V.S. Costa);
0000-0001-9178-0601 (L.H. Macedo);
0000-0002-0683-3914 (E.V. Fortes)

been gaining emphasis, being possible to mention the works of Dey et al. [7], Kairuz et al. [8], Najson [9], and Poonawala [10].

Among the control methods applied to switched linear systems, the predictive approach stands out. In this context, it is worth mentioning the research involving the works of Hall and Bridgeman [11], Marcolino et al. [12]. In Hall and Bridgeman [11], the authors develop a study about exogenous switching in the context of switched predictive control, and in Marcolino et al. [12], the authors explore the application of predictive control and the switching action between two or more control laws designed through linearized processes as a function of structured uncertainties.

Similarly, the works of Kiani et al. [13], Liu et al. [14], Monasterios and Trodden [15] can be mentioned. In Kiani et al. [13], the authors propose a robust switched predictive control for controlling generators in wind energy applications. In Liu et al. [14], a switched predictive control approach is proposed for the actuation of permanent magnet synchronous motor drives, ensuring a fixed switching frequency while preserving the dynamics of the predictive control. Finally, in Monasterios and Trodden [15], the feasibility of implementing decentralized predictive control to switched linear systems is discussed.

Still, in the scope of predictive control, it is possible to mention the works of Barzegarkhoo et al. [16], Sleiman et al. [17]. In Barzegarkhoo et al. [16], the authors control the current injection in electrical distribution networks by three-phase inverters and apply predictive control associated with the switching operation among different control arrangements. In Sleiman et al. [17], the authors propose the implementation of a switched model predictive control (MPC) method for controlling the speed and position of robots.

Finally, we highlight the works of Nabais and Lemos [18], Khan et al. [19]. In Nabais and Lemos [18], the synthesis of adaptive predictive control based on multiple linear subsystems is proposed, where the local control laws incorporate a model-based predictive control algorithm, and the global control action is determined by a switching rule. In the Khan et al. [19], a switched predictive control method is applied to a seven-level three-phase single-source inverter topology for grid-connected photovoltaic applications.

Motivated by the aforementioned different switched predictive control approaches, in this paper, a synthesis of a robust model-based predictive controller for switched discrete linear systems, called switched robust model predictive control (SR-MPC), is proposed.

The proposed method is an extension of the control strategy proposed by Wan and Kothare [20, 21] and the switching rule defined by Geromel and Colaneri [22, 23]. These works, use linear matrix inequalities (LMIs) to solve their respective modeling and optimization problems.

The offline design of the proposed control approach seeks the minimization of the upper bound of the quadratic performance index to an infinite horizon (IH), associated with the switched state estimator and the switching rule, seeking to guarantee closed-loop robust stability of the system.

The main contributions of this work are highlighted below:

1. A synthesis of controllers by state and output feedback via robust MPC with a switching approach, is developed. The proposed model has the advantage that it can be implemented in both online and offline arrangements via look-up table (LUT). To the best of the authors' knowledge, such an approach has not yet been presented in the literature;

2. A model stability analysis using stability ellipsoids with emphasis on offline design via LUT is proposed, inspired by Wan and Kothare [20, 21]. Moreover, an input and output stability analysis of the controller-observer is conducted. The advantage of this approach is that it ensures the robustness of the closed-loop output feedback design along with the best performance obtained through the stability ellipsoids and the observer structure.

The main novelty of this study consists of a robust switched controller-observer model-based predictive control design using an LMI approach summarized in an algorithm, in which feedback controller gains and the ellipsoids boundaries are stored in the LUT along with the observer gains for each user-defined subsystem. Differently from what was proposed in Benallouch et al. [24], in this paper, an evaluation of the performance of the proposed controller by switching between the subsystems and the control action is performed. The evaluation method is performed using nonintrusive performance indices and the temporal response of the closed-loop system. Moreover, unlike the works verified in the literature, in this paper, an iterative method is proposed with a switching approach that follows the principle of invariant stability ellipsoids for switched systems. To validate the proposal, three theorems are formulated: in the first one, the design of the control by state feedback is formalized; in the second theorem, the design of the state observer is idealized; and in the third theorem, the stability of the controller-observer set is characterized.

The remainder of this paper is organized as follows: in Section 2, definitions and an overview of the proposed SR-MPC control technique and the switching rule are presented, based on the works of Wan and Kothare [20, 21], Geromel and Colaneri [22, 23]. In Section 3, the application of the proposed control method is performed in two distinct plants, and a comparative analysis is carried out between the control strategy proposed in this work and the one presented in Benallouch et al. [24]. Finally, in Section 4, the conclusions of the study and proposals for future work are presented.

2. Problem Statement

For the synthesis of an output feedback control, both in online and offline arrangements, three steps must be followed. In the first step, the state feedback gain, which will be described in Theorem 1, is determined. In the second step, a state estimator, which can be verified in Theorem 2, is independently designed. Finally, in the third step, the stabilizability and robustness of the combined observer-controller set are verified, as will be described in Theorem 3.

2.1. Initial Considerations

Initially, consider a linear system subject to switching, as shown in (1).

$$\begin{cases} \boldsymbol{x}(k+1) = \boldsymbol{A}_{\boldsymbol{\sigma}(k)}\boldsymbol{x}(k) + \boldsymbol{B}_{\boldsymbol{\sigma}(k)}\boldsymbol{u}(k) + \boldsymbol{W}_{\boldsymbol{\sigma}(k)}\boldsymbol{w}(k) \\ \boldsymbol{z}(k) = \boldsymbol{C}_{\boldsymbol{\sigma}(k)}\boldsymbol{x}(k) + \boldsymbol{D}_{\boldsymbol{\sigma}(k)}\boldsymbol{u}(k) \end{cases} \tag{1}$$

In (1), $\boldsymbol{x}(k) \in \mathbb{R}^n$ are the states of the system, $\boldsymbol{u}(k) \in \mathbb{R}^m$ is the control signal, $\boldsymbol{z}(k) \in \mathbb{R}^q$ is the output signal, and $\boldsymbol{w}(k) \in \mathbb{R}^r$ is the system disturbance, defined in (2). Moreover, $\boldsymbol{A}$ is the state matrix, $\boldsymbol{B}$ is the input matrix, $\boldsymbol{W}$ is the disturbance matrix, $\boldsymbol{C}$ is the output matrix, and $\boldsymbol{D}$ is the direct transition matrix. All these matrices vary according to the switching rule that, at each time instant, selects a given local model from the set composed of the N subsystems, which describe the dynamics of the global model, available for the switching action, as expressed in (2) and (3).

$$\mathbb{W} = \left\{ \boldsymbol{w} \in \mathbb{R}^r \;\middle|\; \|\boldsymbol{W}\|_{\mathcal{L}_2^r} \leq w_{\max} \right\} \tag{2}$$

$$\boldsymbol{\sigma}(k) \in \mathbb{N},\ \ \mathbb{N} = \{1\,,2\,,\ldots,\ N\}\,,\ \ \forall\ \ k \geq 0 \tag{3}$$

Based on Geromel and Colaneri [22, 23], the Lyapunov stability criterion for switched systems is assumed, as shown in (4), and the switching rule is considered, as shown in (5).

$$\boldsymbol{V}\left(\boldsymbol{x}(k|k), \boldsymbol{\sigma}(k)\right) = \boldsymbol{x}(k|k)^T \boldsymbol{P}_{\boldsymbol{\sigma}(k)}\boldsymbol{x}(k|k) \tag{4}$$

$$\boldsymbol{\sigma}(\boldsymbol{x}(k)) = \arg \min_{\boldsymbol{\sigma}(k)\,=\,i\,\in\,\mathbb{N}} \boldsymbol{x}(k|k)^T \boldsymbol{P}_{\boldsymbol{\sigma}(k)}\boldsymbol{x}(k|k) \tag{5}$$

In (4) and (5), $\boldsymbol{P}_{\boldsymbol{\sigma}(k)}$ is the stability matrix of the respective subsystem and the notation $\boldsymbol{x}(k_1|k_2)$ corresponds to the system states at time k_1 predicted from time k_2. Equations (4) and (5) denote the application of Lyapunov's stability criterion to a given switched system and the switching rule, respectively. The notation $\boldsymbol{\sigma}(k)$ indicates that the respective matrix is subject to switching at each instant of time k. The switching signal depends on the system states and the project follows the procedure proposed by Geromel and Colaneri [22, 23].

Moreover, suppose that there are constraints imposed on the control signal and the behavior of the states, as described, respectively, in (6) and (7).

$$\mathbb{U} = \left\{\boldsymbol{u}(k) : -\boldsymbol{u}_{\text{lim}}^{z_d} \leq \boldsymbol{u}^{z_d}(k) \leq \boldsymbol{u}_{\text{lim}}^{z_d},\ z_d = 1,\ 2,\ \ldots,\ m\right\} \tag{6}$$

$$\mathbb{X} = \left\{\boldsymbol{x}(k) : -\boldsymbol{x}_{\text{lim}}^{v_d} \leq \boldsymbol{x}^{v_d}(k) \leq \boldsymbol{x}_{\text{lim}}^{v_d},\ v_d = 1,\ 2,\ \ldots,\ n\right\} \tag{7}$$

In (6) and (7), z_d is the size of the input signal array and v_d is the size of the state array on the z-plane. For the synthesis of the SR-MPC, consider the quadratic performance index to an IH, as proposed by Benallouch et al. [24], expressed in (8).

$$\boldsymbol{J}_\infty(k) = \sum_{k=0}^{\infty} \left(\|\boldsymbol{x}(k)\|^2_{\boldsymbol{R}_x} + \|\boldsymbol{u}(k)\|^2_{\boldsymbol{R}_u} - \lambda^2 \|\boldsymbol{w}(k)\|^2_{\boldsymbol{R}_w} \right) \tag{8}$$

In (8), $\boldsymbol{u}(k)$ is the control signal for the system, $\boldsymbol{x}(k)$ and $\boldsymbol{w}(k)$ are the predicted state variables and the exogenous noise variables, respectively. $\boldsymbol{J}_\infty(k)$ is the quadratic cost function at time k over an infinite horizon to an implicit function of the sequences of switching signals of the model, $\lambda > 0$ is known as the noise attenuation constant, $\boldsymbol{R}_x = \boldsymbol{C}^T_{\boldsymbol{\sigma}(k)}\boldsymbol{C}_{\boldsymbol{\sigma}(k)} > \boldsymbol{0}$, $\boldsymbol{R}_u = \boldsymbol{D}^T_{\boldsymbol{\sigma}(k)}\boldsymbol{D}_{\boldsymbol{\sigma}(k)} > \boldsymbol{0}$, and $\boldsymbol{R}_w > \boldsymbol{0}$.

2.2. Synthesis of the Controller

From the considerations presented in Subsection 2.1, Theorem 1 is proposed.

Theorem 1. *Consider the switched system defined in (1), subject to (5) − (7), and a control law* $\boldsymbol{u}(k) = \boldsymbol{F}_{\boldsymbol{\sigma}(k)}\boldsymbol{x}(k)$ *with* $\boldsymbol{F}_{\boldsymbol{\sigma}(k)} = \boldsymbol{X}_{\boldsymbol{\sigma}(k)}\boldsymbol{G}_{\boldsymbol{\sigma}(k)}^{-1}$*. It is possible to determine* $\boldsymbol{F}_{\boldsymbol{\sigma}(k)} \in \left\{\boldsymbol{F}_1,\ \boldsymbol{F}_2,\ \ldots,\ \boldsymbol{F}_N\right\}$ *(state feedback gains) and* $\boldsymbol{G}_{\boldsymbol{\sigma}(k)} \in \left\{\boldsymbol{G}_1,\ \boldsymbol{G}_2,\ \ldots,\ \boldsymbol{G}_N\right\}$ *(stability matrices) for each available subsystem during the switching process, if any* $\boldsymbol{S}_{\boldsymbol{\sigma}(k)} = \boldsymbol{S}_{\boldsymbol{\sigma}(k)}^T \geq \boldsymbol{0}$*,* $\boldsymbol{G}_{\boldsymbol{\sigma}(k)} \geq \boldsymbol{0}$*,* $\boldsymbol{V}_{\boldsymbol{\sigma}(k)} > \boldsymbol{0}$*,* $\boldsymbol{X}_{\boldsymbol{\sigma}(k)} > \boldsymbol{0}$*,* $\boldsymbol{Z}_{\boldsymbol{\sigma}(k)} > \boldsymbol{0}$*,* $\eta > 0$*, and* $\mu > 0$ *exist, such that the optimization process (9) − (13) is feasible.*

$$\min_{\boldsymbol{S}_{\boldsymbol{\sigma}},\, \boldsymbol{G}_{\boldsymbol{\sigma}},\, \boldsymbol{X}_{\boldsymbol{\sigma}}} \eta \tag{9}$$

subject to:

$$\begin{bmatrix} \boldsymbol{G}_i + \boldsymbol{G}_i^T - \boldsymbol{S}_i & * & * & * \\ \boldsymbol{A}_i\boldsymbol{G}_i + \boldsymbol{B}_i\boldsymbol{X}_i & \boldsymbol{S}_j & * & * \\ \boldsymbol{C}_i\boldsymbol{G}_i + \boldsymbol{D}_i\boldsymbol{X}_i & \boldsymbol{0} & \eta\boldsymbol{I} & * \\ \boldsymbol{0} & \eta\boldsymbol{W}_i^T & \boldsymbol{0} & \eta\mu\boldsymbol{R}_w \end{bmatrix} \geq \boldsymbol{0} \tag{10}$$

$$\begin{bmatrix} 1 & * & * \\ \mu w_{\max}^2 & \eta\mu w_{\max}^2 & * \\ \boldsymbol{x}(k|k) & \boldsymbol{0} & \boldsymbol{S}_i \end{bmatrix} \geq \boldsymbol{0} \tag{11}$$

$$\begin{bmatrix} \boldsymbol{Z}_i & * \\ \boldsymbol{X}_i & \boldsymbol{G}_i + \boldsymbol{G}_i^T - \boldsymbol{S}_i \end{bmatrix} \geq \boldsymbol{0} \tag{12}$$

$$\begin{bmatrix} \boldsymbol{V}_i & * & * \\ \boldsymbol{A}_i\boldsymbol{G}_i + \boldsymbol{B}_i\boldsymbol{X}_i & \omega_{\max}^{-1}\left(\boldsymbol{G}_i + \boldsymbol{G}_i^T - \boldsymbol{S}_i\right) & * \\ \boldsymbol{W}_i & \boldsymbol{0} & \omega_{\max}^{-1}\boldsymbol{I} \end{bmatrix} \geq \boldsymbol{0} \tag{13}$$

In Theorem 1, $\boldsymbol{Z}_i^{z_d} \leq \left(u_{\text{lim}}^{z_d}\right)^2$ and $\boldsymbol{V}_i^{v_d} \leq \left(x_{\text{lim}}^{v_d}\right)^2$. Moreover, the norm-limited disturbance is described by $w_{\max}$ and $\omega_{\max} = 1 + w_{\max}^2$. The attenuation constant and the upper bound of the performance index are given, respectively, by $\lambda = \sqrt{\mu}$ and $\beta = \sqrt{\eta}$. It is worth mentioning that the proposed optimization process can be performed as a function of μ or η, and to avoid issues related to bilinear terms, η or μ are treated as the objective function and as a design parameter, respectively.

Proof. See Appendix A. □

Regarding the LMIs present in the minimization process described in Theorem 1, it is worth emphasizing that the control law $\boldsymbol{u}(k) = \boldsymbol{F}_{\boldsymbol{\sigma}(k)}\boldsymbol{x}(k)$, with $\boldsymbol{F}_{\boldsymbol{\sigma}(k)} = \boldsymbol{X}_{\boldsymbol{\sigma}(k)}\boldsymbol{G}_{\boldsymbol{\sigma}(k)}^{-1}$, follows directly from LMI (10) and it guarantees the stability of the system subject to switching (1) by minimizing the performance index (8). However, it does not guarantee the robustness of the system during the control action.

To solve this problem, the design method proposed by Kothare et al. [25] was adopted, according to which, the existence of invariant ellipsoids limiting the behavior of the states on the plane composed by them guarantee the robustness of the control action for the entire iterative process.

Varying as a function of the switching rule (5), the stability ellipsoids, subject to the switching between the L subsystems, available in the course of the switching action, can be defined by (14).

$$\epsilon = \left\{ \boldsymbol{x} \in \mathbb{R}^n \;\middle|\; \boldsymbol{x}^T\boldsymbol{G}_{\boldsymbol{\sigma}(k)}^{-1}\boldsymbol{x} \leq 1 \right\} \tag{14}$$

The use of the artifice shown in (14) in the synthesis of the controller results in the formulation of the LMI (11), being one of the greatest advantages of this work in comparison to the one developed by Benallouch et al. [24], whose control strategy considers only the ellipsoid corresponding to the initial condition of the system. By considering not only the initial condition in the iterative process, but also the values of the states of the system for each instant of time, the proposed method guarantees the robustness of the model for the entire iterative process regardless of the initial condition, in addition to enable the model to be implemented online.

Finally, it is worth noting that the LMIs (12) and (13) correspond, respectively, to the constraints of the control signal and the behavior of the states (6) and (7), associated with the switching rule (5). The proposed model makes the closed-loop system globally asymptotically stable.

2.3. Online and Offline Algorithms

The SR-MPC, characterized by Theorem 1, can be implemented under two distinct arrangements: the online and the offline SR-MPC. In the online arrangement, the gain of the controller is determined automatically at each sampling instant. This implies an increasing computational effort as the complexity of the processes increases [20, 21].

The offline arrangement consists of obtaining the control law using interpolations over a LUT based on the existence of the stability ellipsoids initially proposed by Kothare et al. [25]. Furthermore, the offline model allows the simplification of the control law for which it is sufficient to insert the LUT into a given microcontroller, for practical applications.

Algorithms 1 and 2, respectively, didactically indicate the implementation method of the online and offline arrangements of the SR-MPC proposed in this paper.

Algorithm 1. ***Online SR-MPC***

Consider an initial condition $\boldsymbol{x}(0)$, such that it satisfies $\|\boldsymbol{x}(0)\|^2_{\boldsymbol{G}^{-1}_{\boldsymbol{\sigma}(0)}} \leq 1$.

Let $k \leftarrow 1$, then follow the steps:

I From Theorem 1, determine the state feedback gain and stability matrix that describe the stability ellipsoid that circumscribes the system states at instant k.

II While $k \leq k_{\text{end}}$, check if the states of the system satisfy the condition $\|\boldsymbol{x}(k)\|^2_{\boldsymbol{G}^{-1}_{\boldsymbol{\sigma}(k)}} \leq 1$.

$i -$ If they satisfy, stop the iterative process;

$ii -$ If they do not satisfy, let $k \leftarrow k+1$ and return to Step $\boldsymbol{I}$.

Algorithm 2. ***Offline SR-MPC***

Consider an initial condition based on the impulse response $\boldsymbol{x}_{\text{set}} \in \mathbb{X}^s$.

Admit a sequence of minimizers (Theorem 1): η_k or μ_k, $\boldsymbol{S}_k$, $\boldsymbol{G}_k$, $\boldsymbol{X}_k$, $\boldsymbol{Z}_k$, and $\boldsymbol{V}_k$, for $k = 1, 2, 3, \ldots, k_s$, subject to (4) – (7) and the LMIs (9) – (13).

Let $k \leftarrow 1$, then follow the steps:

I Evaluate the minimizers η_k or μ_k, $\boldsymbol{S}_k$, $\boldsymbol{G}_k$, $\boldsymbol{X}_k$, $\boldsymbol{Z}_k$, and $\boldsymbol{V}_k$ applying the additional constraint $\boldsymbol{G}_{k-1} > \boldsymbol{G}_k$ (ignore for $k = 1$) and accumulate $\boldsymbol{G}_k^{-1}$ and $\boldsymbol{X}_i$ in the LUT.

II While $k \leq k_s$, check if the states $\boldsymbol{x}_{k+1}$ satisfy the condition $\left\|\boldsymbol{x}_{k+1}\right\|^2_{\boldsymbol{G}^{-1}_{\boldsymbol{\sigma}(k)}} \leq 1$.

$i -$ If they satisfy, stop the iterative process;

$ii -$ If they do not satisfy, let $k \leftarrow k+1$ and return to Step $\boldsymbol{I}$.

III If $k > k_s$, apply the control law $\boldsymbol{u}(k) = \boldsymbol{F}_{\boldsymbol{\sigma}(k)}\boldsymbol{x}(k)$, where $\boldsymbol{F}_{\boldsymbol{\sigma}(k)} = \boldsymbol{X}_{\boldsymbol{\sigma}(k)}\boldsymbol{G}^{-1}_{\boldsymbol{\sigma}(k)}$, calculated from the LUT constructed in the previous steps.

2.4. State Observer

Aiming at the synthesis of the robust state observer via LMIs applied to the switched system (1), it is necessary to consider the estimated system (15) and, from the superposition principle [1], Theorem 2 is proposed.

$$\begin{cases} \hat{\boldsymbol{x}}(k+1) = \boldsymbol{A}_{\boldsymbol{\sigma}(k)}\hat{\boldsymbol{x}}(k) + \boldsymbol{B}_{\boldsymbol{\sigma}(k)}\boldsymbol{u}(k) + \boldsymbol{W}_{\boldsymbol{\sigma}(k)}\boldsymbol{w}(k) + \boldsymbol{L}_{\boldsymbol{\sigma}(k)}\left(\boldsymbol{z}(k) - \hat{\boldsymbol{z}}(k)\right) \\ \hat{\boldsymbol{z}}(k) = \boldsymbol{C}_{\boldsymbol{\sigma}(k)}\hat{\boldsymbol{x}}(k) + \boldsymbol{D}_{\boldsymbol{\sigma}(k)}\boldsymbol{u}(k), \quad \hat{\boldsymbol{x}}(0) = 0 \end{cases} \tag{15}$$

Theorem 2. *Consider the estimated system (15) subject to the switching rule (5) and the rate of decay of the estimation error ξ $(0 < \xi < 1)$. Then, it is possible to determine the state estimation $\boldsymbol{L}_{\boldsymbol{\sigma}(k)} \in \left\{L_1, L_2, \ldots, L_N\right\}$ where $\boldsymbol{L}_{\boldsymbol{\sigma}(k)} = \boldsymbol{G}^{-1}_{\boldsymbol{\sigma}(k)}\boldsymbol{Y}_{\boldsymbol{\sigma}(k)}$, if there exist matrices $\boldsymbol{Q}_{\boldsymbol{\sigma}(k)} = \boldsymbol{Q}^T_{\boldsymbol{\sigma}(k)} \geq 0$, $\boldsymbol{G}_{\boldsymbol{\sigma}(k)} \geq 0$, and $\boldsymbol{Y}_{\boldsymbol{\sigma}(k)} > 0$, such that the LMI (16) is satisfied.*

$$\begin{bmatrix} \xi^2(\boldsymbol{G}_i + \boldsymbol{G}_i^T - \boldsymbol{Q}_i) & * \\ \boldsymbol{A}_i\boldsymbol{G}_i - \boldsymbol{C}_i\boldsymbol{Y}_i & \boldsymbol{Q}_i \end{bmatrix} \geq 0 \tag{16}$$

Proof. See Appendix B. □

2.5. Closed-Loop Stability

To verify the closed-loop stability of the controller-observer set applied to the system (1), Theorem 3 is formulated.

Theorem 3. *Consider the state matrix of the model that describes the dynamics between the real and estimated systems, as in* (17)*.*

$$\mathcal{A}_i = \begin{bmatrix} \boldsymbol{A}_{\boldsymbol{\sigma}(k)} & \boldsymbol{B}_{\boldsymbol{\sigma}(k)}\boldsymbol{F}_{\boldsymbol{\sigma}(k)} \\ \boldsymbol{L}_{\boldsymbol{\sigma}(k)}\boldsymbol{C}_{\boldsymbol{\sigma}(k)} & \boldsymbol{A}_{\boldsymbol{\sigma}(k)} + \boldsymbol{B}_{\boldsymbol{\sigma}(k)}\boldsymbol{F}_{\boldsymbol{\sigma}(k)} - \boldsymbol{L}_{\boldsymbol{\sigma}(k)}\boldsymbol{C}_{\boldsymbol{\sigma}(k)} \end{bmatrix} \tag{17}$$

The observer-controller set, subject to the switching rule (5)*, will be globally asymptotically stable if there exist the state feedback gains* $\boldsymbol{F}_{\boldsymbol{\sigma}(k)}$*, a state estimation gain* $\boldsymbol{L}_{\boldsymbol{\sigma}(k)}$*, characterized, respectively, in Theorems 1 and 2, and matrices* $\mathcal{Q}_{\boldsymbol{\sigma}(k)} = \mathcal{Q}^T_{\boldsymbol{\sigma}(k)} \geq 0$ *and* $\mathcal{G}_{\boldsymbol{\sigma}(k)} \geq 0$ *of appropriate order, such that LMI* (18) *presents a feasible response.*

$$\begin{bmatrix} \mathcal{G}_i + \mathcal{G}_i^T - \mathcal{Q}_i & * \\ \mathcal{A}_i\mathcal{G}_i & \mathcal{G}_i \end{bmatrix} \geq 0 \tag{18}$$

Proof. See Appendix C. □

3. Tests and Results

In this Section, the control theory developed in Section 2 will be applied to two different plants. The objective is to compare the numerical results with those achieved by the method proposed by Benallouch et al. [24]. In all the examples, it is assumed that the system is described by two linear subsystems: $\boldsymbol{\sigma}(1)$, shown in (19) − (21), and $\boldsymbol{\sigma}(2)$, described in (22) − (24).

For validation of the proposed control strategy, two distinct situations are considered: in the first one, the system states are available and, therefore, the control is performed using state feedback (SF). In the second, the system states are not available, and, therefore, it is necessary to implement output feedback (OF) through the proposed switched state observer.

For solving the LMIs, SeDuMi and YALMIP are used, since YALMIP allows problems involving convex programming to be represented in a more natural way in MATLAB, automatically making an interface with SeDuMi [26]. The tests were conducted on a computer with a 2.20 GHz 8$^{\text{th}}$ generation Intel® Core$^{\text{TM}}$ i3 processor and 8 GB of RAM.

3.1. Example I

For the implementation of the first example, consider the parametric model given in (1), where the state, input, output, disturbance, and direct transition matrices are given in (19) − (21) for subsystem $\boldsymbol{\sigma}(1)$ and matrices (22) − (24) will be used for subsystem $\boldsymbol{\sigma}(2)$.

$$\boldsymbol{A}_1 = \begin{bmatrix} -0.050 & 0.000 & 0.10 & 0.00 \\ 0.000 & -0.300 & 0.00 & 0.10 \\ -0.125 & 0.125 & 0.00 & 0.00 \\ 0.125 & -0.125 & 0.00 & -0.15 \end{bmatrix} \tag{19}$$

$$\boldsymbol{B}_1 = \begin{bmatrix} 0.20 \\ 0.80 \\ 0.00 \\ 0.10 \end{bmatrix} \quad \boldsymbol{W}_1 = \begin{bmatrix} 0.05 \\ 0.03 \\ 0.02 \\ 0.03 \end{bmatrix} \tag{20}$$

$$\boldsymbol{C}_1 = \boldsymbol{I}_{4\times4}, \quad \boldsymbol{D}_1 = \boldsymbol{0} \tag{21}$$

$$\boldsymbol{A}_2 = \begin{bmatrix} -0.150 & 0.060 & 0.30 & -0.06 \\ 0.000 & -0.900 & 0.00 & 0.30 \\ -0.375 & 0.375 & 0.00 & 0.00 \\ 0.375 & -0.375 & 0.00 & -0.45 \end{bmatrix} \tag{22}$$

$$\boldsymbol{B}_2 = \begin{bmatrix} 0.60 \\ 2.40 \\ 0.00 \\ 0.30 \end{bmatrix} \quad \boldsymbol{W}_2 = \begin{bmatrix} 0.03 \\ 0.09 \\ 0.06 \\ 0.15 \end{bmatrix} \tag{23}$$

Table 1
Look-Up Table Obtained for Example I

x_1^{set}	$\boldsymbol{\sigma}(1)$	$\boldsymbol{\sigma}(2)$
1.00	$\boldsymbol{F} = [-0.0166\ 0.5080\ 0.0608\ -0.0401]$	$\boldsymbol{F} = [-0.0080\ 0.4925\ 0.0831\ -0.0372]$
0.50	$\boldsymbol{F} = [-0.0166\ 0.5082\ 0.0608\ -0.0401]$	$\boldsymbol{F} = [-0.0080\ 0.4924\ 0.0831\ -0.0371]$
0.30	$\boldsymbol{F} = [-0.0166\ 0.5081\ 0.0604\ -0.0402]$	$\boldsymbol{F} = [-0.0080\ 0.4924\ 0.0832\ -0.0372]$
0.20	$\boldsymbol{F} = [-0.0166\ 0.5088\ 0.0609\ -0.0399]$	$\boldsymbol{F} = [-0.0080\ 0.4922\ 0.0833\ -0.0371]$
0.15	$\boldsymbol{F} = [-0.0166\ 0.5084\ 0.0608\ -0.0400]$	$\boldsymbol{F} = [-0.0080\ 0.4923\ 0.0833\ -0.0371]$
0.10	$\boldsymbol{F} = [-0.0166\ 0.5085\ 0.0608\ -0.0401]$	$\boldsymbol{F} = [-0.0080\ 0.4924\ 0.0833\ -0.0372]$
0.07	$\boldsymbol{F} = [-0.0166\ 0.5084\ 0.0608\ -0.0401]$	$\boldsymbol{F} = [-0.0080\ 0.4926\ 0.0832\ -0.0372]$
0.05	$\boldsymbol{F} = [-0.0166\ 0.5086\ 0.0608\ -0.0401]$	$\boldsymbol{F} = [-0.0080\ 0.4925\ 0.0832\ -0.0372]$
0.035	$\boldsymbol{F} = [-0.0166\ 0.5089\ 0.0607\ -0.0399]$	$\boldsymbol{F} = [-0.0080\ 0.4920\ 0.0834\ -0.0372]$
0.001	$\boldsymbol{F} = [-0.0166\ 0.5121\ 0.0612\ -0.0388]$	$\boldsymbol{F} = [-0.0080\ 0.4914\ 0.0836\ -0.0372]$

$$\boldsymbol{C}_2 = \boldsymbol{I}_{4\times4}, \quad \boldsymbol{D}_2 = \boldsymbol{0} \tag{24}$$

The initial condition for obtaining the time response for the simulated cases is given in (25).

$$\boldsymbol{X}(0) = \begin{bmatrix} 1.00 & -1.00 & 0.00 & 0.00 \end{bmatrix}^T \tag{25}$$

To perform a comparative analysis between the cited methods, both models were submitted to the same switching sequence, shown in Fig. 1, determined by the switching rule, characterized in (5). In this context, it is important to note that in Benallouch et al. [24], the authors did not evidence the switching sequence of the proposed model.

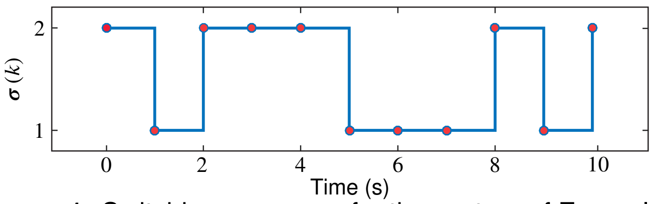

Figure 1: Switching sequence for the system of Example I.

By assuming the presence of a gaussian noise signal with standard deviation of 1.2 and $\boldsymbol{R}_w = \boldsymbol{I}_{1\times1}$, the same excitation vector based on the impulse response adopted by Wan and Kothare [21], and constraints imposed on the input signal and states, $u_{\lim}^{z_d} = 1.0$ and $x_{\lim}^{v_d} = 1.0$, it was possible to construct the LUT (for SF) for $\boldsymbol{\sigma}(1)$ and $\boldsymbol{\sigma}(2)$, as shown in Table 1.

Fig. 2 presents the stability ellipsoids related to the interaction of the states of each subsystem, constructed from the stability matrix $\boldsymbol{G}_i^{-1}$, the excitation vector x_1^{set}, and Table 1.

According to Wan and Kothare [21], the stability matrix corresponds to an ellipsoidal set on the plane composed of the interaction of the system states and tends to the origin of the plane in steady-state as the system reaches asymptotic stability, a fact observed in all the stability ellipsoids illustrated in Fig. 2.

In Fig. 3, the process of minimizing the objective function for the presented problem is illustrated. As previously discussed, for the solution of the LMIs that describe the proposed control, it is necessary to fix μ or η when searching for the optimal solution, thus avoiding issues related to bilinear terms. For the simulation of Example I, the value of $\mu = \sqrt{0.3}$ was fixed when η was minimized.

In Fig. 4 and Fig. 5, it is possible to observe, respectively, the states of the system and the state feedback control signal. In both cases, the curves in red are from the control strategy presented by Benallouch et al. [24], while those in blue are the result of the proposed model.

When simulating the second implementation condition, with OF, which considers the nonavailability of the system states for state feedback, two sets of gains for the switched-state observer are obtained, with a decay rate of the estimation error defined as $\xi = 0.1$, as per (26) and (27).

$$\boldsymbol{L}_{\boldsymbol{\sigma}(1)} = \begin{bmatrix} -0.4070 & -2.1655 & 0.9328 & -1.4922 \end{bmatrix}^T \tag{26}$$
$$\boldsymbol{L}_{\boldsymbol{\sigma}(2)} = \begin{bmatrix} -1.4676 & -8.4352 & 4.0131 & -7.1576 \end{bmatrix}^T \tag{27}$$

Fig. 6 and Fig. 7 show, respectively, the estimated states of the system and the control signal via output feedback. When analyzing the curves and comparing them with the response of the system via state feedback

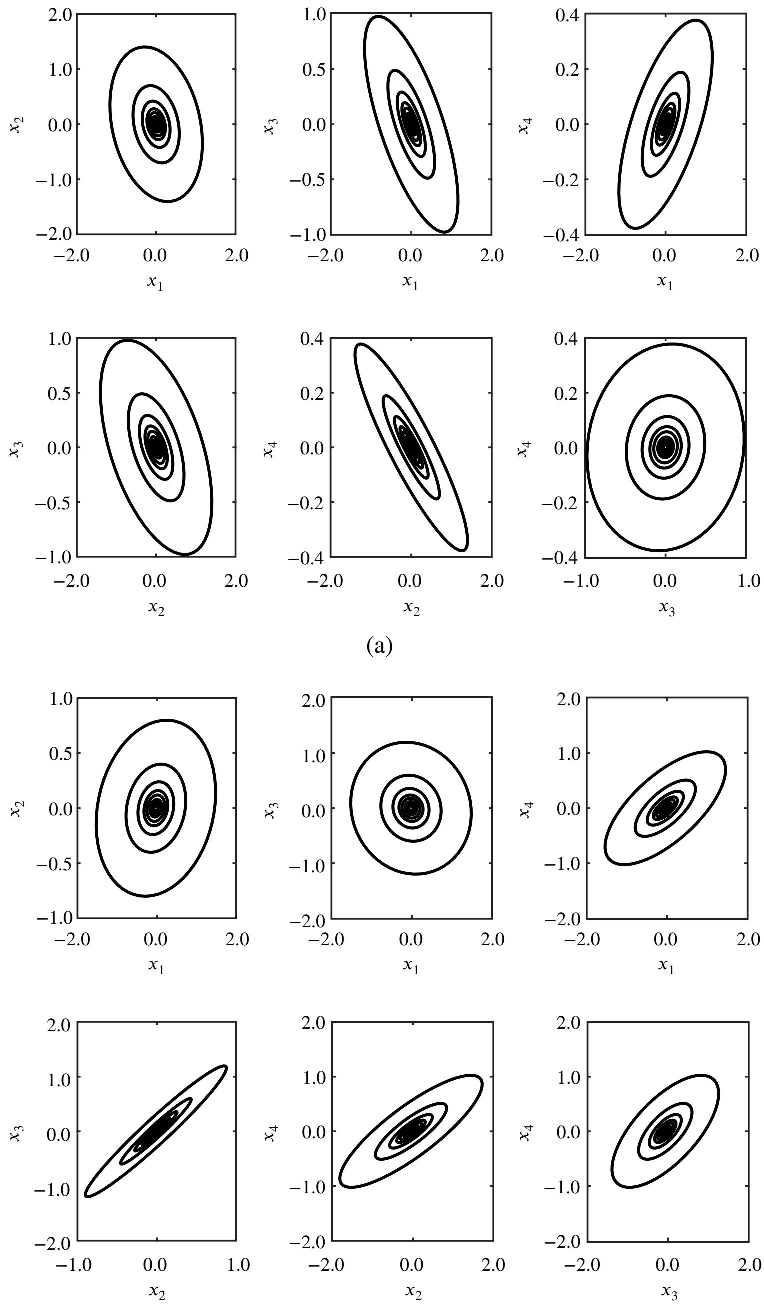

(a)

(b)

Figure 2: Stability ellipsoids for (a) subsystem 1 and (b) subsystem 2 of Example I.

(Fig. 4 and Fig. 5), it is verified that the time response of the controller-observer model presents smaller amplitudes, both in the behavior of the states and in the control signal. It is worth noting that the estimated model was also subjected to the same switching action illustrated in Fig. 1.

To perform a quantitative analysis of the efficiency of the presented arrangements, the nonintrusive performance indices discussed in Shinners [27] were used, according to which, the closer the index is to zero, the greater is the efficiency of the simulated control. In Table 2, the indices integral absolute error (IAE), integral squared error (ISE), integral time-weighted absolute error (ITAE), and integral of time multiplied square error (ITSE), obtained from the implemented models, are presented.

In Table 2, in red, are the performance indices obtained from the proposal of Benallouch et al. [24], in black, the indices referring to the proposed strategy for the SF case, and, in blue, the indices for the proposed strategy for the OF case. By analyzing Table 2, it is possible to observe that the offline SR-MPC controllers, SF and OF, presented better results when these are compared with the results obtained from the control strategy proposed in Benallouch et al. [24]. Moreover, the OF control strategy presented the best indices.

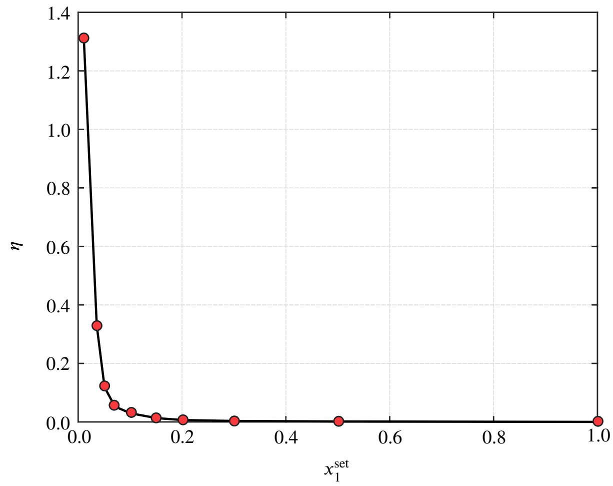

Figure 3: Minimization of η for $\mu = \sqrt{0.3}$, Example I.

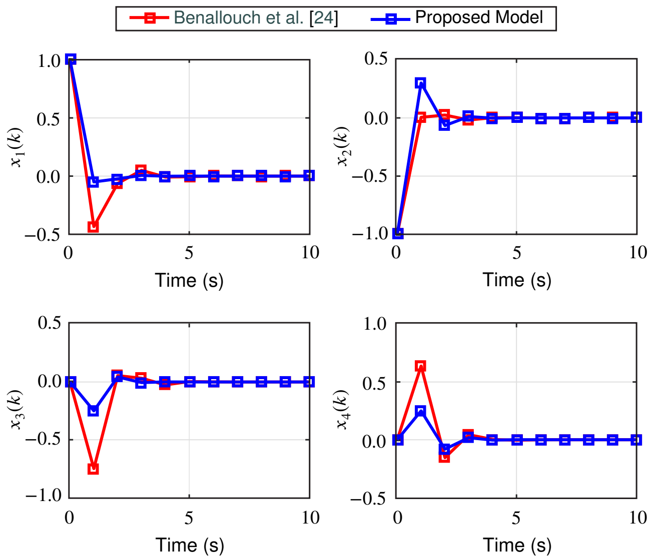

Figure 4: System behavior with state feedback control for Example I.

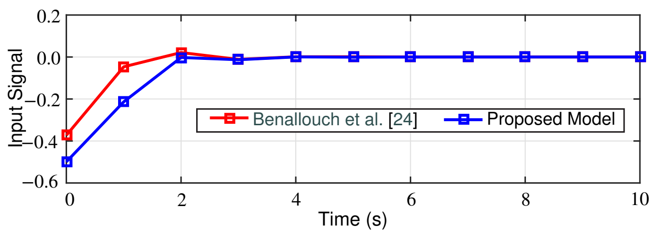

Figure 5: State feedback control signal for Example I.

3.2. Example II

For the implementation of the second example, consider the parametric model given in (1), where the model matrices, for the two subsystems, and the initial condition, are given, respectively, in (28) – (31) and (32).

$$\boldsymbol{A}_1 = \begin{bmatrix} 0.28 & 0.06 \\ 0.10 & 0.14 \end{bmatrix} \boldsymbol{B}_1 = \begin{bmatrix} 0.02 \\ 0.10 \end{bmatrix} \boldsymbol{W}_1 = \begin{bmatrix} 0.02 \\ 0.03 \end{bmatrix} \tag{28}$$

$$\boldsymbol{C}_1 = \boldsymbol{I}_{2\times 2}, \quad \boldsymbol{D}_1 = \boldsymbol{0} \tag{29}$$

$$\boldsymbol{A}_2 = \begin{bmatrix} -0.5 & 0.2 \\ -1.2 & 0.4 \end{bmatrix} \boldsymbol{B}_2 = \begin{bmatrix} 0.80 \\ 1.20 \end{bmatrix} \boldsymbol{W}_2 = \begin{bmatrix} 0.30 \\ 0.40 \end{bmatrix} \tag{30}$$

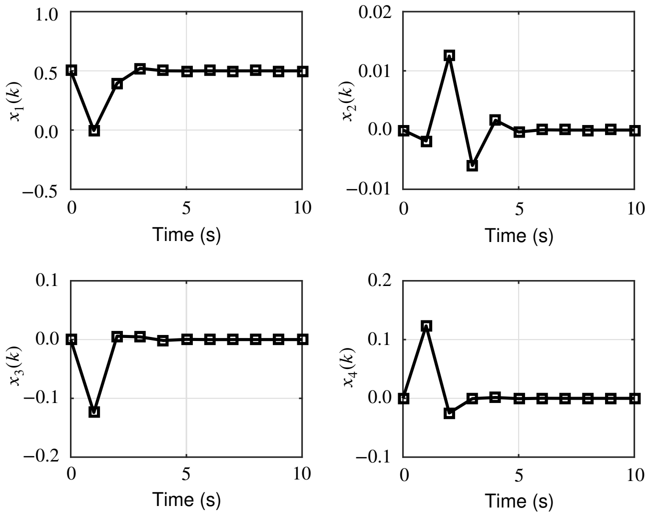

Figure 6: System behavior with output feedback control for Example I.

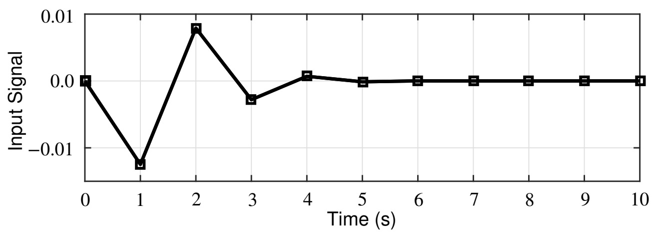

Figure 7: Control signal from the observer-controller system of Example I.

Table 2
Performance Indices for Example I

	Benallouch et al. [24]	Proposed SF	Proposed OF
IAE	3.3241	2.1123	0.3726
ISE	2.1960	1.2314	0.0341
ITAE	3.0974	1.4330	0.4734
ITSE	1.2416	0.2458	0.0352

$$C_2 = I_{2\times 2}, \quad D_2 = \mathbf{0} \tag{31}$$

$$X(0) = \begin{bmatrix} 1.0 & -1.0 \end{bmatrix}^T \tag{32}$$

As in Example I, both models were subjected to the same optimal switching sequence, shown in Fig. 8, determined by the switching rule defined by (5).

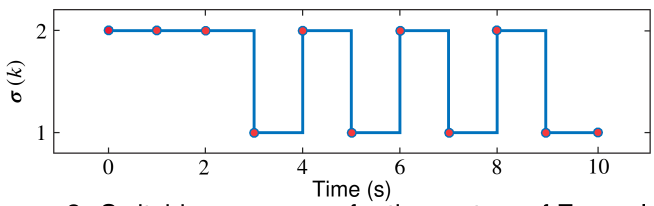

Figure 8: Switching sequence for the system of Example II.

To implement the numerical simulations for Example II, the same parameters and disturbances applied to Example I were adopted, with a single difference that the standard deviation of the gaussian noise signal for this case is 2.2. From the above, Table 3 presents the LUT (for SF) obtained for $\boldsymbol{\sigma}(1)$ and $\boldsymbol{\sigma}(2)$.

In Fig. 9 (a) and Fig. 9 (b), the stability ellipsoids referring to the interaction of the states of each subsystem are illustrated, constructed from the stability matrix $\boldsymbol{G}_i^{-1}$ and the excitation vector x_1^{set}, presented in Table 3.

Table 3
Look-Up Table Obtained for Example II

x_1^{set}	$\sigma(1)$	$\sigma(2)$
1.00	$\boldsymbol{F} = 1 \times 10^{-5}$ [0.0001 0.0006]	$\boldsymbol{F} = [0.8715 \ -0.0119]$
0.50	$\boldsymbol{F} = 1 \times 10^{-5}$ [0.0004 0.0078]	$\boldsymbol{F} = [0.8716 \ -0.0117]$
0.30	$\boldsymbol{F} = 1 \times 10^{-5}$ [0.0002 0.0033]	$\boldsymbol{F} = [0.8718 \ -0.0116]$
0.20	$\boldsymbol{F} = 1 \times 10^{-5}$ [0.0017 0.0339]	$\boldsymbol{F} = [0.8720 \ -0.0115]$
0.15	$\boldsymbol{F} = 1 \times 10^{-5}$ [0.0002 0.0034]	$\boldsymbol{F} = [0.8717 \ -0.0120]$
0.10	$\boldsymbol{F} = 1 \times 10^{-5}$ [0.0008 0.0164]	$\boldsymbol{F} = [0.8721 \ -0.0117]$
0.07	$\boldsymbol{F} = 1 \times 10^{-5}$ [0.0021 0.0416]	$\boldsymbol{F} = [0.8717 \ -0.0115]$
0.05	$\boldsymbol{F} = 1 \times 10^{-5}$ [0.0016 0.0330]	$\boldsymbol{F} = [0.8711 \ -0.0120]$
0.035	$\boldsymbol{F} = 1 \times 10^{-5}$ [0.0011 0.0230]	$\boldsymbol{F} = [0.8710 \ -0.0113]$
0.001	$\boldsymbol{F} = 1 \times 10^{-5}$ [−0.018 0.3443]	$\boldsymbol{F} = [0.8717 \ -0.0118]$

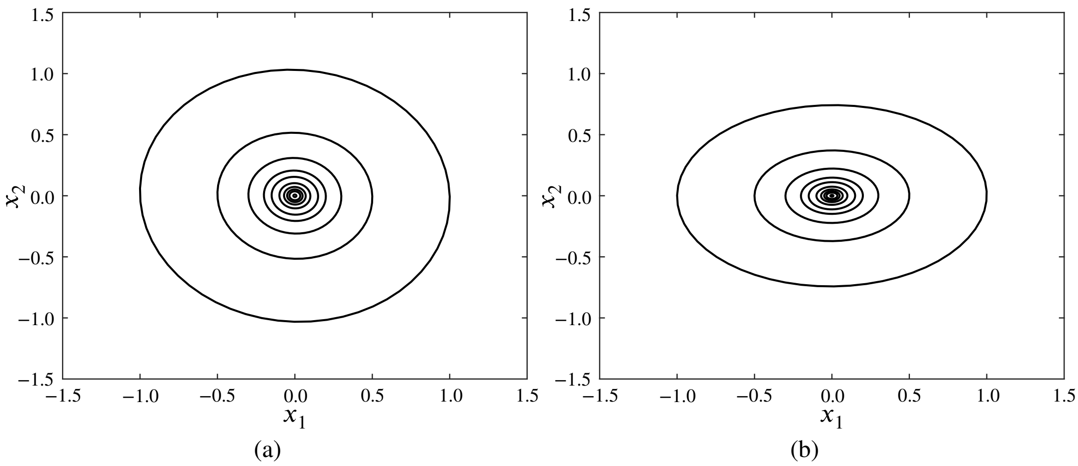

Figure 9: Stability ellipsoids for (a) subsystem 1 and (b) subsystem 2 of Example II.

Fig. 10 illustrates the temporal dynamics of Fig. 9. These refer to the simulated optimization process for the offline algorithm.

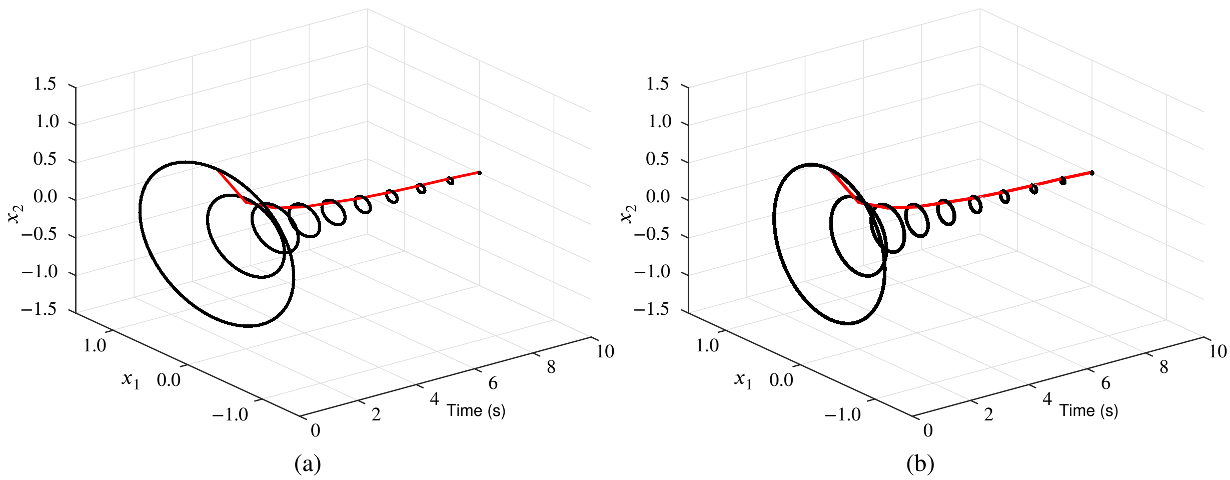

Figure 10: 3-D stability ellipsoids for (a) subsystem 1 and (b) subsystem 2 of Example II.

By analyzing Fig. 9 and Fig. 10, it can be observed that, in both cases, the ellipsoids converge to the center and tend to the origin of the plane in the steady-state. Moreover, the excitation vector x_1^{set} (red curve) remains within the region bounded by the stability ellipsoids, a fact that implies the robustness of the system and, consequently, the optimal convergence of the algorithm [25].

In Fig. 11, the minimization process of the objective function of the set of LMIs, (9) − (13), is presented. In the simulation, the value of $\mu = \sqrt{0.2828}$ was fixed and the minimization of η was sought for the offline process.

By analyzing Fig. 9 to Fig. 11 and Table 3, it is possible to observe the overview of the convergence process of the proposed algorithm in a detailed way, since it is possible to associate each line of the LUT to

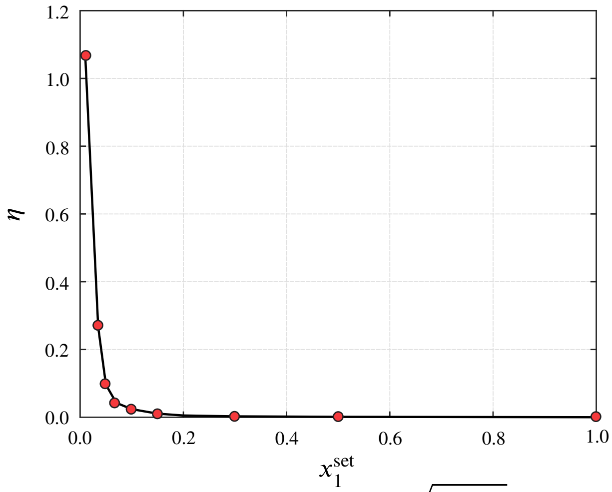

Figure 11: Minimization of η for $\mu = \sqrt{0.2828}$, Example II.

each element of x_1^{set} and the respective stability ellipsoid and verify the robustness of the process according to the criteria described in Kothare et al. [25].

From the state feedback gains shown in Table 3, it is possible to obtain Fig. 12, which shows the behavior of the system states, and Fig. 13, that shows the control signal via state feedback.

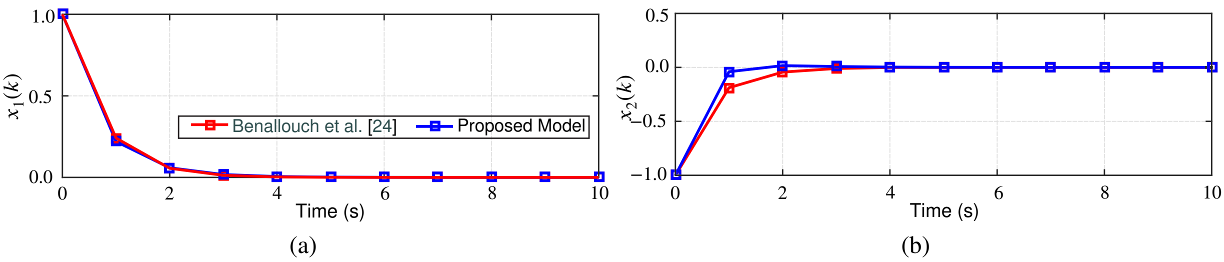

Figure 12: System behavior with state feedback control for Example II for (a) $x_1(k)$ and (b) $x_2(k)$.

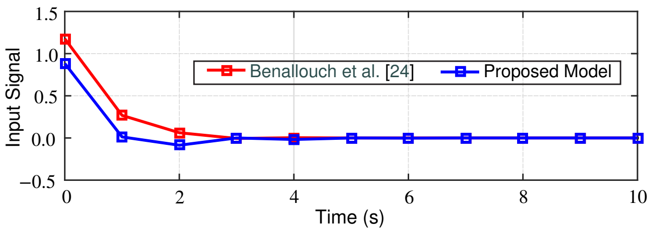

Figure 13: State feedback control signal of Example II.

In Fig. 12 and Fig. 13, the red curves are from the control strategy presented by Benallouch et al. [24], while the blue curves are obtained from the proposed method. It can be verified that, in both figures, the system response via SF using the proposed method was very close to that presented by Benallouch et al. [24]. However, further analysis using performance indices will show that the strategy addressed in this work is more efficient.

When simulating the second implementation condition, with OF, i.e., considering the nonavailability of system states for state feedback, two sets of gains for the switched-state observer are obtained, (33) and (34), with an estimation error decay rate $\xi = 0.1$.

$$\boldsymbol{L}_{\boldsymbol{\sigma}(1)} = \begin{bmatrix} 0.1723 & -0.0381 \end{bmatrix}^T \tag{33}$$

$$\boldsymbol{L}_{\boldsymbol{\sigma}(2)} = \begin{bmatrix} 0.1196 & -0.1455 \end{bmatrix}^T \tag{34}$$

Fig. 14 and Fig. 15 show the estimated system states and the control signal via output feedback, respectively.

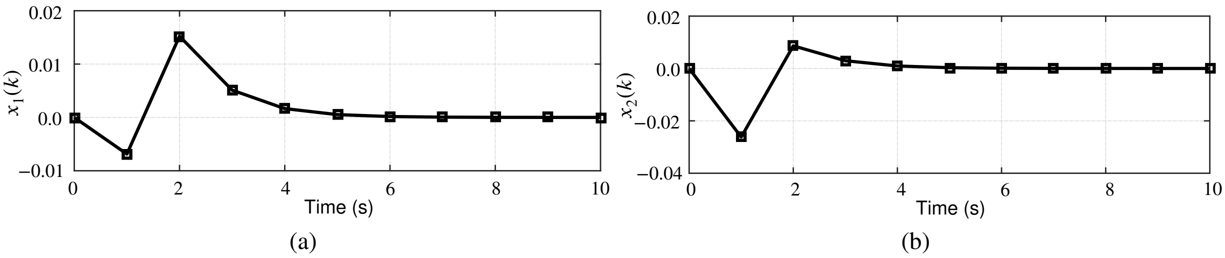

Figure 14: System behavior with output feedback control for Example II for (a) $x_1(k)$ and (b) $x_2(k)$.

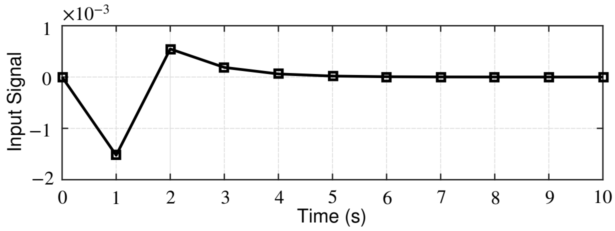

Figure 15: Control signal from the observer-controller system of Example II.

Table 4
Performance Indices for Example II

	Benallouch et al. [24]	Proposed SF	Proposed OF
IAE	1.5567	1.3735	0.0688
ISE	1.0989	1.0542	0.0011
ITAE	0.7186	0.5427	0.1908
ITSE	0.1045	0.0588	0.0025

By analyzing Fig. 14 and Fig. 15, it is possible to infer that, as in Example I, the response of the observer-controller set also presented lower amplitudes, both in the behavior of the states and in the control signal.

Finally, a quantitative analysis of the efficiency of the three arrangements presented using the nonintrusive performance indices IAE, ISE, ITAE, and ITSE, is performed. The results of this analysis are shown in Table 4.

In Table 4, the results described in red, black, and blue are characterized exactly as they were defined for Table 2. When analyzing Table 4, it is possible to observe that the offline SR-MPC controllers, SF and OF, presented better results when these are compared with the results obtained from the control strategy of Benallouch et al. [24]. Again, the OF control strategy presented the best indices.

4. Conclusion

In this paper, three theorems were formulated for the synthesis of robust model predictive control (RMPC) and a state observer, both designed via linear matrix inequalities and applied to switched linear systems. In addition, the proposed control was implemented in the offline arrangement, since the online model requires more computational effort, which makes its application for higher complexity or high order systems infeasible.

To determine which control strategy (state feedback or output feedback) via switched robust-model predictive control (SR-MPC) is more efficient, a series of comparative analysis between the proposed models and a benchmark, using two different plants, were performed. It is worth mentioning that, among the analyzed characteristics, emphasis was given to the time responses of the systems under gaussian disturbances, nonintrusive performance indices, and robustness analysis via stability ellipsoids.

In view of the obtained results, it was verified that the proposed control strategies presented better performance than the benchmark method in all examples and simulated cases, with emphasis on the output feedback control arrangement.

As a proposal for future work, there is the possibility of developing research both in modeling and simulation, as well as for applications in experimental problems. In these cases, it is possible to develop studies involving modeling of the proposed control for linear parameter varying systems and for systems whose uncertainties are polytopically modeled, both subject to switching, and applications of SR-MPC for the control of electromagnetic power converters, such as the buck and boost converters.

A. Proof of Theorem 1

Proof. Suppose that (1) can be rearranged as a closed-loop system, as described in (35).

$$\begin{cases} \boldsymbol{x}(k+1) = \left(\boldsymbol{A}_{\boldsymbol{\sigma}(k)} + \boldsymbol{B}_{\boldsymbol{\sigma}(k)}\boldsymbol{F}_{\boldsymbol{\sigma}(k)}\right)\boldsymbol{x}(k) + \boldsymbol{W}_{\boldsymbol{\sigma}(k)}\boldsymbol{w}(k) \\ \boldsymbol{z}(k) = \left(\boldsymbol{C}_{\boldsymbol{\sigma}(k)} + \boldsymbol{D}_{\boldsymbol{\sigma}(k)}\boldsymbol{F}_{\boldsymbol{\sigma}(k)}\right)\boldsymbol{x}(k) \end{cases} \tag{35}$$

From (35), it is possible to obtain the state and output matrices of the closed-loop model given, respectively, in (36) and (37).

$$\bar{\boldsymbol{A}}_{\boldsymbol{\sigma}(k)} = \boldsymbol{A}_{\boldsymbol{\sigma}(k)} + \boldsymbol{B}_{\boldsymbol{\sigma}(k)}\boldsymbol{F}_{\boldsymbol{\sigma}(k)} \tag{36}$$

$$\bar{\boldsymbol{C}}_{\boldsymbol{\sigma}(k)} = \boldsymbol{C}_{\boldsymbol{\sigma}(k)} + \boldsymbol{D}_{\boldsymbol{\sigma}(k)}\boldsymbol{F}_{\boldsymbol{\sigma}(k)} \tag{37}$$

To minimize the performance index defined in (8) it is necessary to apply the concepts of H_∞ norm filtering, Lyapunov stability, defined in (4), and use (36) and (37) in (35) to formulate the inequality (38), based on the same principle adopted by Benallouch et al. [24] and Kothare et al. [25].

$$\begin{gathered} \boldsymbol{x}(k)^T\left(\bar{\boldsymbol{A}}_{\boldsymbol{\sigma}(k)}^T\boldsymbol{P}_{\boldsymbol{\sigma}(k+1)}\bar{\boldsymbol{A}}_{\boldsymbol{\sigma}(k)} - \boldsymbol{P}_{\boldsymbol{\sigma}(k)} + \bar{\boldsymbol{C}}_{\boldsymbol{\sigma}(k)}^T\bar{\boldsymbol{C}}_{\boldsymbol{\sigma}(k)}\right)\boldsymbol{x}(k) + \boldsymbol{w}(k)^T\left(\boldsymbol{W}_{\boldsymbol{\sigma}(k)}^T\boldsymbol{P}_{\boldsymbol{\sigma}(k+1)}\boldsymbol{W}_{\boldsymbol{\sigma}(k)} - \lambda^2\boldsymbol{R}_w\right)\boldsymbol{w}(k) + \\ 2\boldsymbol{x}(k)^T\left(\bar{\boldsymbol{A}}_{\boldsymbol{\sigma}(k)}^T\boldsymbol{P}_{\boldsymbol{\sigma}(k+1)}\boldsymbol{W}_{\boldsymbol{\sigma}(k)}\right)\boldsymbol{w}(k) \leq \boldsymbol{0} \end{gathered} \tag{38}$$

By separating $\boldsymbol{x}(k)^T$ and $\boldsymbol{w}(k)^T$ on the left-hand side, and $\boldsymbol{x}(k)$ and $\boldsymbol{w}(k)$ on the right-hand side, it is possible to rewrite (38) into (39).

$$\begin{bmatrix} \bar{\boldsymbol{A}}_{\boldsymbol{\sigma}(k)}^T\boldsymbol{P}_{\boldsymbol{\sigma}(k+1)}\bar{\boldsymbol{A}}_{\boldsymbol{\sigma}(k)} - \boldsymbol{P}_{\boldsymbol{\sigma}(k)} + \bar{\boldsymbol{C}}_{\boldsymbol{\sigma}(k)}^T\bar{\boldsymbol{C}}_{\boldsymbol{\sigma}(k)} & * \\ \bar{\boldsymbol{A}}_{\boldsymbol{\sigma}(k)}^T\boldsymbol{P}_{\boldsymbol{\sigma}(k+1)}\boldsymbol{W}_{\boldsymbol{\sigma}(k)} & \boldsymbol{W}_{\boldsymbol{\sigma}(k)}^T\boldsymbol{P}_{\boldsymbol{\sigma}(k+1)}\boldsymbol{W}_{\boldsymbol{\sigma}(k)} - \lambda^2\boldsymbol{R}_w \end{bmatrix} \leq \boldsymbol{0} \tag{39}$$

By applying Schur complement to (39) and rearranging the inequality, it is possible to formulate (40).

$$\begin{bmatrix} \boldsymbol{P}_{\boldsymbol{\sigma}(k)} & * & * & * \\ \bar{\boldsymbol{A}}_{\boldsymbol{\sigma}(k)}\boldsymbol{P}_{\boldsymbol{\sigma}(k+1)} & \boldsymbol{P}_{\boldsymbol{\sigma}(k+1)} & * & * \\ \bar{\boldsymbol{C}}_{\boldsymbol{\sigma}(k)} & 0 & \boldsymbol{I} & * \\ \boldsymbol{0} & \boldsymbol{W}_{\boldsymbol{\sigma}(k)}^T\boldsymbol{P}_{\boldsymbol{\sigma}(k+1)} & \boldsymbol{0} & \lambda^2\boldsymbol{R}_w \end{bmatrix} \geq \boldsymbol{0} \tag{40}$$

For simplicity, let $i = \boldsymbol{\sigma}(k)$, $j = \boldsymbol{\sigma}(k+1)$, $\mu = \lambda^2$, $\boldsymbol{P}_i = \eta\boldsymbol{S}_i^{-1}$, and $\boldsymbol{P}_j = \eta\boldsymbol{S}_j^{-1}$ in (40). From the above, by inspection, it is possible to obtain (41).

$$\begin{bmatrix} \eta\boldsymbol{S}_i^{-1} & * & * & * \\ \bar{\boldsymbol{A}}_i\eta\boldsymbol{S}_j^{-1} & \eta\boldsymbol{S}_j^{-1} & * & * \\ \bar{\boldsymbol{C}}_i & \boldsymbol{0} & \boldsymbol{I} & * \\ \boldsymbol{0} & \boldsymbol{W}_i^T\eta\boldsymbol{S}_j^{-1} & \boldsymbol{0} & \mu\boldsymbol{R}_w \end{bmatrix} \geq \boldsymbol{0} \tag{41}$$

By applying the relaxation concept proposed by Cuzzola et al. [28], it is possible to assume the existence of an invertible matrix $\boldsymbol{G}$ of appropriate order, and it is possible to pre and post multiply this matrix in (41) by the diagonal block $\mathbb{B} = \text{bdiag}\left(\boldsymbol{G}_i^T,\ \boldsymbol{S}_j,\ \eta,\ \eta\right)$. Therefore, it is possible to rewrite it as (42).

$$\begin{bmatrix} \boldsymbol{G}_i + \boldsymbol{G}_i^T - \boldsymbol{S}_i & * & * & * \\ \boldsymbol{G}_i\bar{\boldsymbol{A}}_i & \boldsymbol{S}_j & * & * \\ \boldsymbol{G}_i\bar{\boldsymbol{C}}_i & \boldsymbol{0} & \eta\boldsymbol{I} & * \\ \boldsymbol{0} & \eta\boldsymbol{W}_i^T & \boldsymbol{0} & \eta\mu\boldsymbol{R}_w \end{bmatrix} \geq \boldsymbol{0} \tag{42}$$

By using (36) and (37) in (42) and performing the substitution $\boldsymbol{X}_i = \boldsymbol{F}_i\boldsymbol{G}_i$, it is possible to complete the proof of the LMI (10).

To ensure the asymptotic stability of the closed-loop system at each sampling instant, consider the optimization problem (43), subject to the stability condition (44).

$$\min_{\boldsymbol{P}_i,\ \beta^2} \beta^2 \tag{43}$$

$$\boldsymbol{x}(k|k)^T\boldsymbol{P}_i\boldsymbol{x}(k|k) + \lambda^2\boldsymbol{w}_{\max}^2 \leq \beta^2 \tag{44}$$

From (44), by inspection, it is possible to obtain (45), where $\boldsymbol{P}_i = \eta\boldsymbol{S}_i^{-1}$, $\eta = \beta^2$, and $\mu = \lambda^2$.

$$1 - \boldsymbol{x}(k|k)^T \boldsymbol{S}_i^{-1} \boldsymbol{x}(k|k) - \eta^{-1} \mu \boldsymbol{w}_{\max}^2 \geq \mathbf{0} \tag{45}$$

By rearranging and applying Schur complement on (45), it is possible to complete the proof of the LMI (11).

To formulate the LMIs (12) and (13), it must be guaranteed that constraints (6) and (7) are satisfied. In this case, the same procedures used by Kothare et al. [25] and Benallouch et al. [24] were adopted. First, to aggregate control input constraints, consider that the Euclidean norm of the signal is less than or equal to the maximum allowed signal, as expressed in (46) − (50).

$$\|\boldsymbol{u}^{z_d}(k)\|_2^2 \leq u_{\text{lim}}^{z_d}, \quad \forall k \geq 0, \quad z_d = 1, 2, \dots m \tag{46}$$

$$\max_{k \geq 0} \|\boldsymbol{u}(k)\|_2^2 = \max_{k \geq 0} \|\boldsymbol{F}_i \boldsymbol{x}(k)\|_2^2 \tag{47}$$

$$= \max_{k \geq 0} \left\| \boldsymbol{X}_i \boldsymbol{G}_i^{-1} \boldsymbol{x}(k) \right\|_2^2 \tag{48}$$

$$\leq \max_{\boldsymbol{x} \in \epsilon} \left\| \boldsymbol{X}_i \boldsymbol{G}_i^{-1} \boldsymbol{x} \right\|_2^2 \tag{49}$$

$$= \lambda_{\max} \left[\left(\boldsymbol{X}_i \boldsymbol{G}_i^{-1} \right)^T \boldsymbol{S}_i^{1/2} \boldsymbol{S}_i^{1/2} \left(\boldsymbol{X}_i \boldsymbol{G}_i^{-1} \right) \right] \tag{50}$$

In (46) − (50), ϵ is an ellipsoidal set defined in (14), and these equations are formulated following the procedure proposed by Kothare et al. [25] to ensure the condition $\|\boldsymbol{u}(k)\|_2^2 \leq \left(u_{\text{lim}}^{z_d}\right)^2$, allowing to obtain (51).

$$\left(u_{\text{lim}}^{d}\right)^2 - \boldsymbol{X}_i^T \left(\boldsymbol{G}_i^T \boldsymbol{S}_i^{-1} \boldsymbol{G}_i \right)^{-1} \boldsymbol{X}_i \geq \mathbf{0} \tag{51}$$

By applying Schur complement to inequality (51), the relaxation method of Cuzzola et al. [28], and assuming the existence of a positive semidefinite variable, $\boldsymbol{Z}_i \leq \left(u_{\text{lim}}^{z_d}\right)^2$, where $z_d = 1, 2, \dots, m$, it is possible to formulate (52), concluding the proof of the LMI (12).

$$\begin{bmatrix} \boldsymbol{Z}_i & * \\ \boldsymbol{X}_i & \boldsymbol{G}_i + \boldsymbol{G}_i^T - \boldsymbol{S}_i \end{bmatrix} \geq \mathbf{0} \tag{52}$$

Given that the norm of the system states is less than or equal to the maximum allowed signal, as described in Benallouch et al. [24], the system states can be written as (53) − (56).

$$\|\boldsymbol{x}^{v_d}(k+1)\|_2^2 \leq x_{\text{lim}}^{v_d}, \quad \forall k \geq 0, \quad v_d = 1, 2, \dots, n \tag{53}$$

$$\max_{k \geq 0} \|\boldsymbol{x}(k+1)\|_2^2 = \max_{k \geq 0} \left\| \begin{bmatrix} \bar{\boldsymbol{A}}_i & \boldsymbol{W}_i \end{bmatrix} \begin{bmatrix} \boldsymbol{x}(k) \\ \boldsymbol{w}(k) \end{bmatrix} \right\|_2^2 \tag{54}$$

$$= \max_{\boldsymbol{x}, \boldsymbol{w} \in \epsilon} \left\| \begin{bmatrix} \bar{\boldsymbol{A}}_i \boldsymbol{S}_i^{-1/2} & \boldsymbol{W}_i \end{bmatrix} \begin{bmatrix} \boldsymbol{S}_i^{1/2} \boldsymbol{x} \\ \boldsymbol{w} \end{bmatrix} \right\|_2^2 \tag{55}$$

$$= \left(1 + w_{\max}^2\right) \left[\left(\bar{\boldsymbol{A}}_i \boldsymbol{S}_i \right)^T \boldsymbol{S}_i^{-1} \left(\bar{\boldsymbol{A}}_i \boldsymbol{S}_i \right) + \boldsymbol{W}_i^T \boldsymbol{W}_i \right] \tag{56}$$

In (53) − (56), the control signal design condition is given by $\|x(k)\|_2^2 \leq \left(x_{\text{lim}}^{v_d}\right)^2$ and ϵ is an ellipsoidal set defined in (14). From the set (53) − (56), it is possible to obtain (57).

$$\left(x_{\text{lim}}^{v_d}\right)^2 - \left(1 + w_{\max}^2\right) \left[\left(\bar{\boldsymbol{A}}_i \boldsymbol{S}_i \right)^T \boldsymbol{S}_i^{-1} \left(\bar{\boldsymbol{A}}_i \boldsymbol{S}_i \right) + \boldsymbol{W}_i^T \boldsymbol{W}_i \right] \geq \mathbf{0} \tag{57}$$

By applying the relaxation process, (36) and (37), considering that $\boldsymbol{V}_i \leq \left(x_{\text{lim}}^{v_d}\right)^2$ where $v_d = 1, 2, \dots, n$ and, by making $\boldsymbol{X}_i = \boldsymbol{F}_i \boldsymbol{G}_i$ and $\omega_{\max} = 1 + w_{\max}^2$ to apply Schur complement, it is possible to conclude the proof of LMI (13) and Theorem 1.

□

B. Proof of Theorem 2

Proof. The interaction between the real (1) and estimated (15) systems, both subject to the switching rule (5), allows determining the equation of the dynamic error expressed by (58), which will be minimized as the estimated model approaches the temporal dynamics of the real model.

$$\boldsymbol{e}(k+1) = \boldsymbol{x}(k+1) - \hat{\boldsymbol{x}}(k+1) \tag{58}$$

According to Wan and Kothare [21], from the decay rate of the estimation error ξ, the gain of the estimator $\boldsymbol{L}_{\boldsymbol{\sigma}(k)}$ can be defined if there exists a matrix $\boldsymbol{P}_{\boldsymbol{\sigma}(k)} \geq \mathbf{0}$, such that it satisfies inequality (59).

$$\xi^2 \boldsymbol{e}(k)^T \boldsymbol{P}_{\boldsymbol{\sigma}(k)} \boldsymbol{e}(k) \geq \boldsymbol{e}(k+1)^T \boldsymbol{P}_{\boldsymbol{\sigma}(k)} \boldsymbol{e}(k+1) \tag{59}$$

From (58) and (59), by inspection, (60) is obtained.

$$\xi^2 \boldsymbol{P}_{\boldsymbol{\sigma}(k)} - (\boldsymbol{A}_{\boldsymbol{\sigma}(k)} - \boldsymbol{L}_{\boldsymbol{\sigma}(k)} \boldsymbol{C}_{\boldsymbol{\sigma}(k)})^T \boldsymbol{P}_{\boldsymbol{\sigma}(k)} (\boldsymbol{A}_{\boldsymbol{\sigma}(k)} - \boldsymbol{L}_{\boldsymbol{\sigma}(k)} \boldsymbol{C}_{\boldsymbol{\sigma}(k)}) \geq \boldsymbol{0} \tag{60}$$

By letting $\boldsymbol{Q}_{\boldsymbol{\sigma}(k)} = \boldsymbol{P}^{-1}_{\boldsymbol{\sigma}(k)}$, $\boldsymbol{L}_{\boldsymbol{\sigma}(k)} = \boldsymbol{Q}^{-1}_{\boldsymbol{\sigma}(k)} \boldsymbol{Y}_{\boldsymbol{\sigma}(k)}$, and adopting the relaxation method proposed by Cuzzola et al. [28] (multiplying (60) on the left by $\boldsymbol{G}_{\boldsymbol{\sigma}(k)}$ and on the right by $\boldsymbol{G}^T_{\boldsymbol{\sigma}(k)}$), it is possible to rewrite (60) as (61).

$$\xi^2 \boldsymbol{G}_{\boldsymbol{\sigma}(k)} \boldsymbol{Q}^{-1}_{\boldsymbol{\sigma}(k)} \boldsymbol{G}^T_{\boldsymbol{\sigma}(k)} - (\boldsymbol{A}_{\boldsymbol{\sigma}(k)} \boldsymbol{G}_{\boldsymbol{\sigma}(k)} - \boldsymbol{L}_{\boldsymbol{\sigma}(k)} \boldsymbol{C}_{\boldsymbol{\sigma}(k)}) \boldsymbol{Q}^{-1}_{\boldsymbol{\sigma}(k)} (\boldsymbol{A}_{\boldsymbol{\sigma}(k)} \boldsymbol{G}_{\boldsymbol{\sigma}(k)} - \boldsymbol{L}_{\boldsymbol{\sigma}(k)} \boldsymbol{C}_{\boldsymbol{\sigma}(k)})^T \geq \boldsymbol{0} \tag{61}$$

By letting $i = \boldsymbol{\sigma}(k)$ and applying Schur complement to inequality (61), (16) is obtained, thus concluding the proof of Theorem 2. □

C. Proof of Theorem 3

Proof. By considering system (1), the deterministic state estimation model in (15), and Theorem 2, it is possible to formulate (62).

$$\begin{cases} \hat{\boldsymbol{x}}(k+1) = \left(\boldsymbol{A}_{\boldsymbol{\sigma}(k)} - \boldsymbol{L}_{\boldsymbol{\sigma}(k)} \boldsymbol{C}_{\boldsymbol{\sigma}(k)}\right) \hat{\boldsymbol{x}}(k) + \left(\boldsymbol{B}_{\boldsymbol{\sigma}(k)} - \boldsymbol{L}_{\boldsymbol{\sigma}(k)} \boldsymbol{D}_{\boldsymbol{\sigma}(k)}\right) \boldsymbol{u}(k) + \boldsymbol{W}_{\boldsymbol{\sigma}(k)} \boldsymbol{w}(k) + \boldsymbol{L}_{\boldsymbol{\sigma}(k)} \boldsymbol{z}(k) \\ \hat{\boldsymbol{z}}(k) = \boldsymbol{C}_{\boldsymbol{\sigma}(k)} \hat{\boldsymbol{x}}(k) + \boldsymbol{D}_{\boldsymbol{\sigma}(k)} \boldsymbol{u}(k), \quad \hat{\boldsymbol{x}}(0) = \boldsymbol{0} \end{cases} \tag{62}$$

From Theorem 1 it is possible to obtain the control law $\boldsymbol{u}(k) = \boldsymbol{F}_{\boldsymbol{\sigma}(k)} \hat{\boldsymbol{x}}(k)$. By considering $\boldsymbol{D}_{\boldsymbol{\sigma}(k)} \equiv \boldsymbol{0}$, (63) is obtained.

$$\begin{cases} \hat{\boldsymbol{x}}(k+1) = \left(\boldsymbol{A}_{\boldsymbol{\sigma}(k)} + \boldsymbol{B}_{\boldsymbol{\sigma}(k)} \boldsymbol{F}_{\boldsymbol{\sigma}(k)} - \boldsymbol{L}_{\boldsymbol{\sigma}(k)} \boldsymbol{C}_{\boldsymbol{\sigma}(k)}\right) \hat{\boldsymbol{x}}(k) + \boldsymbol{W}_{\boldsymbol{\sigma}(k)} \boldsymbol{w}(k) + \boldsymbol{L}_{\boldsymbol{\sigma}(k)} \boldsymbol{z}(k) \\ \hat{\boldsymbol{z}}(k) = \boldsymbol{C}_{\boldsymbol{\sigma}(k)} \hat{\boldsymbol{x}}(k), \quad \hat{\boldsymbol{x}}(0) = \boldsymbol{0} \end{cases} \tag{63}$$

From (63) and the real closed-loop model (35), it is possible to obtain the augmented model (64).

$$\boldsymbol{\mathcal{X}}(k+1) = \begin{bmatrix} \boldsymbol{A}_{\boldsymbol{\sigma}(\boldsymbol{k})} & \boldsymbol{B}_{\boldsymbol{\sigma}(k)} \boldsymbol{F}_{\boldsymbol{\sigma}(k)} \\ \boldsymbol{L}_{\boldsymbol{\sigma}(k)} \boldsymbol{C}_{\boldsymbol{\sigma}(k)} & \boldsymbol{A}_{\boldsymbol{\sigma}(k)} + \boldsymbol{B}_{\boldsymbol{\sigma}(k)} \boldsymbol{F}_{\boldsymbol{\sigma}(k)} - \boldsymbol{L}_{\boldsymbol{\sigma}(k)} \boldsymbol{C}_{\boldsymbol{\sigma}(k)} \end{bmatrix} \begin{bmatrix} \boldsymbol{x}(k) \\ \hat{\boldsymbol{x}}(k) \end{bmatrix} \tag{64}$$

By subjecting (64) to the Lyapunov stability criterion given in (4), (65) can be formulated, where $\boldsymbol{\mathcal{A}}_{\sigma(k)}$ and $\boldsymbol{\mathcal{P}}_{\sigma(k)}$ are, respectively, the state and stability matrices of the augmented model.

$$\boldsymbol{\mathcal{P}}_{\boldsymbol{\sigma}(k)} - \boldsymbol{\mathcal{A}}^T_{\boldsymbol{\sigma}(k)} \boldsymbol{\mathcal{P}}_{\boldsymbol{\sigma}(k)} \boldsymbol{\mathcal{A}}_{\boldsymbol{\sigma}(k)} \geq \boldsymbol{0} \tag{65}$$

By making $\boldsymbol{\mathcal{P}}_{\boldsymbol{\sigma}(k)} = \boldsymbol{\mathcal{Q}}^{-1}_{\boldsymbol{\sigma}(k)}$, where $\boldsymbol{\mathcal{Q}}_{\boldsymbol{\sigma}(k)} = \boldsymbol{\mathcal{Q}}^T_{\boldsymbol{\sigma}(k)} \geq \boldsymbol{0}$, admitting the existence of a positive invertible and semidefinite $\boldsymbol{\mathcal{G}}_{\boldsymbol{\sigma}(k)}$ and adopting the notation $i = \boldsymbol{\sigma}(k)$, it is possible to rewrite inequality (65) as (66).

$$\mathcal{G}_i^T \mathcal{Q}_i^{-1} \mathcal{G}_i - \left(\mathcal{A}_i \mathcal{G}_i\right)^T \mathcal{G}_i^{-1} \left(\mathcal{A}_i \mathcal{G}_i\right) \geq \boldsymbol{0} \tag{66}$$

By applying the relaxation concepts proposed by Cuzzola et al. [28] and applying Schur complement on (66), it is possible to obtain (18) and, therefore, conclude the proof of Theorem 3.

Hence, the observer-controller set will be globally asymptotically stable if there exist a feedback gain $\boldsymbol{F}_{\boldsymbol{\sigma}(k)}$ and a state estimator $\boldsymbol{L}_{\boldsymbol{\sigma}(k)}$, as well as matrices $\boldsymbol{\mathcal{G}}_i$ and $\boldsymbol{\mathcal{Q}}_i$, such that LMI (18) presents a feasible solution. □

References

[1] Ogata, K.. Modern control engineering. Boston: Prentice-Hall; 2010. ISBN 0136156738.

[2] Teixeira, M., Assuncao, E., Avellar, R.. On relaxed LMI-based designs for fuzzy regulators and fuzzy observers. IEEE Transactions on Fuzzy Systems 2003;11(5):613–623. doi:10.1109/tfuzz.2003.817840.

[3] Castillo, O.. Soft computing for control of non-linear dynamical systems. Heidelberg: Physica-Verlag HD Imprint Physica; 2001. ISBN 978-3-662-00367-1. doi:10.1007/978-3-7908-1832-1.

[4] Braun, S.. Encyclopedia of vibration. San Diego: Academic Press; 2002. ISBN 9780080523620.

[5] Liberzon, D.. Switching in systems and control. Boston: Birkhäuser; 2003. ISBN 978-1-4612-6574-0. doi:10.1007/978-1-4612-0017-8.

[6] Liberzon, D., Morse, A.. Basic problems in stability and design of switched systems. IEEE Control Systems 1999;19(5):59–70. doi:10.1109/37.793443.

[7] Dey, S., Taousser, F.Z., Djemai, M., Defoort, M., Gennaro, S.D.. Observer based leader–follower bipartite consensus with intermittent failures using lyapunov functions and time scale theory. IEEE Control Systems Letters 2021;5(6):1904–1909. doi:10.1109/lcsys.2020.3040944.

[8] Kairuz, R.I.V., Orlov, Y., Aguilar, L.T.. Prescribed-time stabilization of controllable planar systems using switched state feedback. IEEE Control Systems Letters 2021;5(6):2048–2053. doi:10.1109/lcsys.2020.3046682.

[9] Najson, F.. Spectral and convex uniform exponential stability determination in a class of switched linear systems. IEEE Control Systems Letters 2021;5(6):2138–2143. doi:10.1109/lcsys.2020.3045920.

[10] Poonawala, H.A.. Stability analysis of conewise affine dynamical systems using conewise linear Lyapunov functions. IEEE Control Systems Letters 2021;5(6):2126–2131. doi:10.1109/lcsys.2020.3046702.

[11] Hall, R.A., Bridgeman, L.J.. Computationally tractable stability criteria for exogenously switched model predictive control. IEEE Control Systems Letters 2021;5(5):1777–1782. doi:10.1109/lcsys.2020.3043866.

[12] Marcolino, M.H., Galvão, R.K.H., Kienitz, K.H.. Predictive control of linear systems with switched actuators subject to dwell-time constraints. Journal of Control, Automation and Electrical Systems 2020;32(1):1–17. doi:10.1007/s40313-020-00667-9.

[13] Kiani, E., Ganji, B., Taher, S.A.. Model predictive control of switched reluctance generator based on z-source converter for wind power applications. International Transactions on Electrical Energy Systems 2020;30(11):1–16. doi:10.1002/2050-7038.12578.

[14] Liu, X., Zhang, Z., Yang, X., Garcia, C., Rodriguez, J.. Fixed switching frequency predictive control for PMSM drives with guaranteed control dynamics. In: 2020 IEEE 9th International Power Electronics and Motion Control Conference (IPEMC2020-ECCE Asia). IEEE; 2020, p. 3033–3038. doi:10.1109/ipemc-ecceasia48364.2020.9367680.

[15] Monasterios, P.R.B., Trodden, P.A.. Coalitional predictive control: Consensus-based coalition forming with robust regulation. Automatica 2021;125:109380. doi:10.1016/j.automatica.2020.109380.

[16] Barzegarkhoo, R., Khan, S.A., Siwakoti, Y.P., Aguilera, R.P., Lee, S.S., Khana, M.N.H.. Implementation and analysis of a novel switched-boost common-ground five-level inverter modulated with model predictive control strategy. IEEE Journal of Emerging and Selected Topics in Power Electronics 2021;:1–14doi:10.1109/jestpe.2021.3068406.

[17] Sleiman, J.P., Farshidian, F., Minniti, M.V., Hutter, M.. A unified MPC framework for whole-body dynamic locomotion and manipulation. IEEE Robotics and Automation Letters 2021;6(3):4688–4695. doi:10.1109/lra.2021.3068908.

[18] Nabais, M., Lemos, J.M.. Distributed adaptive predictive control based on switched multiple models and ADMM. In: Lecture Notes in Electrical Engineering. Springer International Publishing; 2020, p. 253–262. doi:10.1007/978-3-030-58653-9_24.

[19] Khan, S.A., Guo, Y., Khan, M.N.H., Siwakoti, Y., Zhu, J., Blaabjerg, F.. A novel single source three phase seven-level inverter topology for grid-tied photovoltaic application. In: 2020 IEEE 9th International Power Electronics and Motion Control Conference (IPEMC2020-ECCE Asia). IEEE; 2020, p. 372–376. doi:10.1109/ipemc-ecceasia48364.2020.9367731.

[20] Wan, Z., Kothare, M.V.. Robust output feedback model predictive control using off-line linear matrix inequalities. Journal of Process Control 2002;12(7):763–774. doi:10.1016/s0959-1524(02)00003-3.

[21] Wan, Z., Kothare, M.V.. An efficient off-line formulation of robust model predictive control using linear matrix inequalities. Automatica 2003;39(5):837–846. doi:10.1016/s0005-1098(02)00174-7.

[22] Geromel, J.C., Colaneri, P.. Stability and stabilization of continuous-time switched linear systems. SIAM Journal on Control and Optimization 2006;45(5):1915–1930. doi:10.1137/050646366.

[23] Geromel, J.C., Colaneri, P.. Stability and stabilization of discrete time switched systems. International Journal of Control 2006;79(7):719–728. doi:10.1080/00207170600645974.

[24] Benallouch, M., Schutz, G., Fiorelli, D., Boutayeb, M.. H∞ model predictive control for discrete-time switched linear systems with application to drinking water supply network. Journal of Process Control 2014;24(6):924–938. doi:10.1016/j.jprocont.2014.04.008.

[25] Kothare, M., Balakrishnan, V., Morai, M.. Robust constrained model predictive control using linear matrix inequalities. Automatica 1996;32:440 – 444 vol.1. doi:10.1109/ACC.1994.751775.

[26] Lofberg, J.. YALMIP : a toolbox for modeling and optimization in MATLAB. In: 2004 IEEE International Conference on Robotics and Automation (IEEE Cat. No.04CH37508). 2004, p. 284–289. doi:10.1109/CACSD.2004.1393890.

[27] Shinners, S.. Modern control system theory and design. New York: J. Wiley; 1998. ISBN 9780471249061.

[28] Cuzzola, F.A., Geromel, J.C., Morari, M.. An improved approach for constrained robust model predictive control. Automatica 2002;38(7):1183–1189. doi:10.1016/s0005-1098(02)00012-2.